FORMATION OF ENRICHED BLACK TEA EXTRACT LOADED CHITOSAN NANOPARTICLES VIA ELECTROSPRAYING

BY

SAMUEL JAMES HAMMOND

A thesis submitted to the

Graduate School-New Brunswick

Rutgers, The State University of New Jersey

In partial fulfillment of the requirements

For the degree of

Master of Science

Graduate Program in Food Science

Written under the direction of

Qingrong Huang

And approved by

_____

_____

_____

_____

New Brunswick, New Jersey

October 2015

ABSTRACT OF THE THESIS

Formation of Enriched Black Tea Extract Loaded Chitosan Nanoparticles via Electrospraying

by SAMUEL JAMES HAMMOND

Thesis Director:
Qingrong Huang

Creating nanoparticles of beneficial nutraceuticals and pharmaceuticals has had a large surge of research due to the enhancement of absorption and bioavailability by decreasing their size. One of these ways is by electrohydrodynamic atomization, also known as electrospraying. In general, this novel process is done by forcing a liquid through a capillary nozzle and which is subjected to an electrical field. While there are different ways to create nanoparticles, the novel method of electrospraying can be beneficial over other types of nanoparticle formation. Reasons include high control over particle size and distribution by altering electrospray parameters (voltage, flow rate, distance, and time), higher encapsulation efficiency than other methods, and also it is a one step process without exposure to extreme conditions (Gomez-Estaca et. al. 2012, Jaworek and Sobcyzk 2008). The current study aimed to create a chitosan encapsulated theaflavin-2 enriched black tea extract (BTE) nanoparticles via electrospraying. The first step of this process was to create the smallest chitosan nanoparticles possible by altering the

electrospray parameters and the chitosan-acetic acid solution parameters. The solution properties altered include chitosan molecular weight, acetic acid concentration, and chitosan concentration. Specifically, the electrospray parameters such as voltage, flow rate and distance from syringe to collector are the most important in determining particle size. After creating the smallest chitosan particles, the TF-2 enriched black tea extract was added to the chitosan-acetic acid solution to be electrosprayed. The particles were assessed with the following procedures: Atomic force microscopy (AFM) and scanning electron microscopy (SEM) for particle morphology and size, and loading efficiency with ultraviolet–visible spectrophotometer (UV-VIS). Chitosan-BTE nanoparticles were successfully created in a one step process. Diameter of the particles on average ranged from 255 nm to 560 nm. Encapsulation efficiency was above 95% for all but one sample set. Future work includes MTT assay and cellular uptake.

ACKNOWLEDGEMENT AND DEDICATION

First I would like to thank Dr. Qingrong Huang for all his help throughout my M.S. He was always available when I had questions or hit a wall with my research and was very supportive.

Thank you to Dr. Chi-Tang Ho and Dr. Qingli Wu for being members of my Master's thesis committee.

I would like to thank Annie D'Souza who helped me a great deal with my SEM experiments. Also I would like to thank Yike Jiang for helping me with cell studies. And I would like to thank all my lab mates over these last few years. Thank you for support and help along the way.

This Master's thesis is dedicated to my family. Without their encouragement and support I don't think I could have finished. Thank you to my parents, Marla and Sam Hammond, my sisters Blake Hammond and Michelle Ottaviano, and my nephew Jaden Ottaviano. You mean everything to me.

TABLE OF CONTENTS

LIST OF FIGURES

LIST OF TABLES

INTRODUCTION

Nanoparticle Production

Nanoparticles are of particular interest in the food and beverage industry. They can offer unique advantages due to their nano-size including increased bioavailability and unique delivery mechanisms for bioactives in foods. In addition, small particles do not cause any visual effects in beverages, offering a clear finished product even with food additives (Huang Q. , 2012).

Nanoparticle formation has two general methods of creation. The first is bottom-up and the second is top-down. Bottom-up approach is accomplished by self-assembly of small molecules to spontaneously create the nanoparticles such as planar assemblies of cellulose fibers in plant cell walls and protein-polysaccharide coacervates by biopolymer interaction (Huang Q. , 2012).

In the top-down approach, nanoparticles are created from larger materials by a reduction process such as milling, homogenization or aerosol routes (Huang Q. , 2012). Milling involves using solid particles in a ball mill or bead mill in order to mechanically break them down into nano-sizes via stress and shear. This process can be either dry or wet (e.g. using water or food grade vegetable oil as an additive). Homogenization can also be used to create nanoparticles which are based on emulsion or dispersions. Homogenizers that can create nanoparticles are defined as either high sheer, high pressure or ultrasonic. Both of these methods cost a great deal of time and energy to complete. In addition to this, all of these methods, aside from dry milling, have nanoparticles in solution when the procedure is finished. In order to get a dry product,

additional steps are needed to remove the solvent from the nanoparticles. However, using aerosol routes such as spray drying or electrospraying creates nanoparticles in a one step process. Spray dryings' particular drawback is that the compounds being spray dried are subjected to high heat. Therefore, compounds that cannot resist degrading or transforming during this process cannot be used in spray drying. Electrospraying offers a novel method of nanoparticles creation in that is a complete one step process that does not subject the compounds to extreme conditions which could cause degradation.

Electrospraying

Figure 1 shows a basic setup of electrospraying including the main components of the apparatus. Electrospraying is the process in which a liquid is subjected to atomization by electrical forces. In general, this process is done by forcing a liquid through a capillary nozzle and which is connected to an electrical field. The buildup of charge on the surface of the liquid destabilizes the surface and forms a Taylor cone (Salata, 2005). The jet will then form droplets due to the electrical field of the apparatus (Jaworek, 2007; Jaworek & Sobcyzk, 2008) . The droplets that are formed are accelerated by the electrical field toward the grounded collector which acts as a counter electrode (Salata, 2005). The droplets are then collected on a grounded surface that is a specific distance away from the nozzle tip. Depending on the parameters of the electrospray and the properties of the liquid, different modes can be achieved from electrospraying resulting in different droplets.

There are two main categories of modes for electrospraying that are important for the type of droplets that are formed. The first set is dripping modes and the second set is

jet modes. Dripping modes include dripping mode, microdripping mode, spindle mode, and multispindle mode (Jaworek & Krupa, 1999). These different modes lead to regular large drops, fine droplets, and elongated spindles respectively (Jaworek & Sobcyzk, 2008). Jet modes include cone-jet mode, oscillating-jet mode, precession mode, and multijet mode (Jaworek & Krupa, 1999). The difference between these is the movement of the jet during the procedure. A smooth and stable cone is the result from the cone-jet mode (Jaworek & Sobcyzk, 2008). In oscillating mode, the jet will move in its own plane. In precession mode, the jet rotates around the capillary axis (Jaworek & Sobcyzk, 2008). The multi-jet mode is exactly how it sounds; multiple jets are emitted at once from the capillary (Jaworek & Sobcyzk, 2008). These different modes are important because they affect the outcome of the electrospray. They can produce different drop sizes, charges, and spatial distributions (Jaworek & Krupa, 1999). Also, the operation parameters for each mode will be different (e.g., voltage, flow rate) (Jaworek & Krupa, 1999). Voltage applied is a key component to which mode is formed during electrospraying. In general, at lower voltages dripping modes are achieved and when more voltage is applied, jet modes start forming (Jaworek & Krupa, 1999).

Electrospray systems have unique advantages over mechanical atomizers. First, the size of the droplets can range from 10nm to hundreds of micrometers (Jaworek & Sobcyzk, 2008). The ability to tune the particle size over such a large range is one of the major novel functions of electrospraying allowing it to be very specific in its applications. Second, the droplet size can be controlled by the flow rate of the liquid and the voltage applied to the capillary nozzle (Jaworek & Sobcyzk, 2008). These variables are easy to manipulate which allows the user to seamlessly change the outcome of their product that

is being electrosprayed. Third, when the preferred size is found, the size distribution of the droplets can have a very small standard deviation creating a uniform product (Jaworek & Sobcyzk, 2008). Fourth, the droplets are self-dispersing due to their charge so they will not coagulate together (Jaworek & Sobcyzk, 2008). Fifth, a charged spray is much more efficient at depositing on the collector than an uncharged spray (Jaworek & Sobcyzk, 2008). These advantages have led to increasing nanotechnology areas in which electrospraying can be very useful.

Electrospraying has been used in many different aspects of nanotechnology. It can be used for thin film deposits on the micro and nano level, nanoparticle production, and capsule formation of either micro or nano level (Jaworek & Sobcyzk, 2008). In particular, there have been many studies of electrospraying involving the creation of delivery systems for pharmaceuticals, which electrospraying shows great promise. Thien et al. (2012) were able to use electrospray to create chitosan-indomethacin nanoparticles for drug delivery and achieve an average size of 340 nm and test the effects of acetic acid concentration, applied voltage, and solution feeding rate on particle size. They found that with the high encapsulation efficiency and long term release, chitosan can be an effective drug carrier. Lee et al. (2011) were able to encapsulate multiple drugs in a one step process into PLGA-coated particles. In this method, they used a triple coaxial needle to achieve the nanoparticle creation. With this technique, this tri-layered structure was able to release multiple drugs in distinct kinetic phases. Yu et al. (2012) created a microparticle via electrospraying using Eudragit® L-100 as the polymer and Diclofenac Sodium as a model drug. Microparticles were achieved with a size of 1.3±0.7 μm. These particles specifically target the colon for drug delivery by using a pH-dependent sustained

release profile. Xie et al. (2008) used electrospraying to encapsulate protein based drugs. Other methods of protein encapsulation face problems during the primary emulsion which causes protein denaturation and aggregation. With electrospraying using PLGA as a carrier, they were succesful in encapsulating proteins for controlled release drug delviery applications.

There have also been electrospray studies involving the creation of delivery systems for nutraceuticals. Gomez-Estaca et al. (2012) was able to create zein-curcumin nanoparticles via electrospraying. They were able to create nanoparticles ranging from 175-900 nm with encapsulation efficiency around 85-90%. This encapsulation allowed them to achieve a good dispersion in an aqueous food matrix (semi-skimmed milk). Jung et al. (2011) used electrospraying on natural plant extracts to create nanoparticles. This study differs from other studies in that no shell or carrier was used. The plant extract was electrosprayed by itself to create nanoparticles that can be used in other applications such as biomedical engineering. Laelorspoen et al. (2014) were able to encapsulate *Lactobacillus acidophilus* with citric acid modified zein. This encapsulation inreased the survival rate of the bacteria in gastric fluid so that it can reach the colon and act as a probiotic. They showed that the encpsulated bacteria only had a 1-log reduction after two hours of incubation compared to the 5-log reduction of bacteria that was not encapsulated.

Particularly in the case of nanoencapsulation and nanoparticle formation, electrospraying has advantages over traditional methods which could potentially make it a much better option for both. Electrospraying has much higher encapsulation efficiency than other methods (Gomez-Estaca, Balaguer, Gavara, & Hernandez-Munoz, 2012). It

has even been reported in other studies have reached an encapsulation efficiency of 80 to 96% (Ding, Lee, & Wang, 2005; Xie, Marijnissen, & Wang, 2006). Encapsulation efficiency is very important when making delivery systems. Higher encapsulation efficiency means less wasted materials and greater production of active particles.

By altering the parameters of the electrospray machine, it is easy to obtain different sized particles with a very narrow distribution in size (Jaworek & Sobcyzk, 2008; Gomez-Estaca, Balaguer, Gavara, & Hernandez-Munoz, 2012). The two most important parameters that affect the size of the particles are voltage applied and flow rate. By altering these parameters, even just slightly, it is possible to change the created particle size while still having a narrow distribution. This is also very important when selecting an encapsulation method because having particles of a particular and uniform size allows greater control over the end product.

Electrospraying is also a one step process, meaning the particle formation and solvent removal is done simultaneously. This is done during the electrospray process itself which reduces the steps and processing needed to form dry particles. This unique advantage is one of the main reasons electrospraying is being used as a novel method of nanoparticle creation. It eliminates a costly and time inefficient step that most nanoparticle creation methods have to do (i.e. remove solvent from nanoparticles after creation). These advantages, most notably being a one-step process, are the main reasons for selecting electrospraying to nanoparticles for delivering pharmaceuticals and nutraceuticals.

Chitosan

Chitosan is a polysaccharide consisting of 2-amino-2-deoxy-β-d-glucan combined with glycosidic linkages. This unique polysaccharide is made from the deacetylation of chitin, a common byproduct of the seafood industry from crustaceans such as shrimp (Dodane & Vilivalam, 1998; Agnihotri, Mallikarjuna, & Aminabhavi, 2004; Vani & Shaleesha, 2013). The primary amine group of chitosan, as well as it being a positively charged polymer, gives it important properties that are useful in nutraceutical and pharmaceutical applications, specifically in micro/nanoparticle production.

Chitosan is a popular polymer used for pharmaceuticals and nutraceuticals, especially in micro and nanoparticle systems due to a variety of unique properties. In pharmaceutical and nutraceutical applications, its unique properties include biocompatibility with living tissues showing no signs of allergic reactions or rejection and breaking down to harmless amino sugars over time (Agnihotri, Mallikarjuna, & Aminabhavi, 2004). In micro/nanoparticle systems, unique advantages are the ability to control release, avoiding use of organic solvents during particle production since it can be readily dissolved in acetic acid systems, its free amine groups that can be used for cross linking and mucoadhesive character which allows increased time at the site of absorption (Agnihotri, Mallikarjuna, & Aminabhavi, 2004). In particular, it can increase the bioavailability of nutraceuticals and pharmaceuticals due this unique mucoadhesion property (Dodane & Vilivalam, 1998).

Previous research has used chitosan in electrospraying for nanoparticle production (Zhang & Kawakami, 2010; Hu, Sheng-Feng, Nair, & Wu, 2012). This research includes

testing a variety of parameters solution formulation (i.e. amount of chitosan and solvent used) as well as electrospray parameters (i.e. flow rate and applied voltage). Hu et al (2012) found that chitosan concentration of the solution should be 1% (w/w) for electrospraying and when increasing to 2% to 5%, nanofibers were formed instead of nanoparticles. Zhang and Kawakami (2010) used electrospraying for chitosan as well and found the optimal conditions in which the smallest particles, 124 nm, were formed. Their formulation used mixture of acetic acid at 30% (v/v), chitosan at 10g/L and ethanol at 20% (v/v). They also found that the most important operation parameter was flow rate while the most important solution properties were conductivity and viscosity. Smaller particles were formed with increasing conductivity and decreasing viscosity.

Due to the unique properties and advantages of chitosan, as well as its previous research in electrospraying, it was selected to be the carrier used in this thesis to demonstrate the novel properties of electrospraying.

Black Tea Extract (BTE)

Black tea is a commonly consumed drink around the world. The composition of black tea is important and includes alkaloids, such as caffeine and theobromine, carbohydrates, amino acids, and glycosylated flavanoids. Together these make up 30-40% of the dry mass of black tea. The rest of the 60-70% of the dry mass is polyphenolic fermentation products (Kuhnert, 2010).

Black teas unique polyphenolic compounds exhibit beneficial properties to humans when consumed. The main active polyphenolic compounds in black tea include catechins (e.g. epigallocatechin-3-gallate (EGCG), epigallocatechin (EGC)), theaflavins

(e.g. theaflavin (TF), theaflavin-3-gallate (TF3G)) and thearubigins. Brewed black tea would typically contain 3-10% catechins, 2-6% theaflavins and >20% thearubigins (Damodaran, Parkin, & Fennema, 2008).

Theaflavins are of high interest in black tea and its extract. These compounds are formed by oxidation and polymerization of catechins in black tea during the fermentation process. Specifically, theaflavin-2 (TF-2) has been shown to have anti-cancer properties by inducing apoptosis in colon cancer cell lines (Gosslau, et al., 2011). Theaflavins have also shown to be an anti-inflammatory compound by inhibition of interleukin-8 gene expression (Aneja, Odoms, Denenberg, & Wong, 2004). Black tea has been shown to have antioxidant properties via inhibiting free radical generation, scavenging free radicals, chelating transition metal ions and also inhibiting the pro-oxidative enzymes xanthine oxidase and nitric oxide synthase (Luczaj & Skrzydlewska, 2005). However, bioavailability of theaflavins is not well understood and tends to be low (Gosslau, et al., 2011). To overcome this problem, nanoparticles can be formed with chitosan as a carrier to enhance absorption via two ways. The first is the nano-size of the particles allows absorption to occur more easily and readily. The second is with the chitosan mucoadhesive property, which allows the nanoparticles to have prolonged contact with the intestines where it can be readily absorbed.

Objectives

The current study aimed to demonstrate the novel process of electrospraying in producing nanoparticles and create a black tea extract loaded chitosan nanoparticle with increased biological activity. The novelty of this process includes producing nano-sized

particles with a small standard deviation, tune-ability of the process in producing different sized particles, high encapsulation efficiency, and being a one step process. The final product could potentially be used as a food additive in a functional beverage and is made completely from generally regarded as safe (GRAS) and food grade materials.

MATERIALS AND METHODS

Solution Materials

Final Solutions

Chitosan used in all final solutions had a molecular weight of 130 KDA and was 98% deacetylated. Black tea extract used was WellGen TF-2 Enriched Black Tea Extract (WG0401). The solvent used for all samples was 90 v/v% acetic acid.

Test Solutions

Chitosan of 330 KDA was also tested with preliminary measures to see how the molecular weight of the chitosan affected nanoparticles formation. In addition to this, the acetic acid used was a lower percentage at 50 v/v%.

Electrospray Machine & Parameters

The final electrospray parameters used are as follows unless otherwise specified: voltage of 20 kV, flow rate of 4 µL/min, and travel distance of 10 cm. Samples were collected on aluminum foil unless otherwise specified. Syringes used for all samples were 3 ml in volume with 22 gauge needles.

Atomic Force Microscopy (AFM)

An atomic force microscope (AFM) was used to image the nanoparticles formed to obtain detailed results of the size and structure of the nanoparticles formed. Nanoparticles were directly sprayed onto AFM mica and allowed to air dry for 24 hours before loading into the AFM to ensure all the solvent was evaporated. A Nanoscope IIIa

was used with a JV scanner in tapping mode. Scan rates ranged from 0.70 to 0.80 hertz. Scan sizes used were 10x10 µm, 5x5 µm, and 2x2 µm. Height and phase data was collected for all chitosan and chitosan-BTE nanoparticle samples.

Scanning Electron Microscopy

After using AFM to find the optimal conditions to produce the nanoparticles, a scanning electron microscope was used to obtain detailed images of the nanoparticle structures and to obtain precise measurements of the nanoparticles diameter. SEM was performed at the McLaren Center of Ceramic Research located on Busch campus of Rutgers University. Nanoparticles were sprayed onto aluminum foil and then transferred to SEM sample holders. Before being scanned, samples received a 10nm coat of gold sputter. The parameters for the SEM were an applied voltage of 5 kV, magnification of 20,000x, and a working distance of 1-2 nm. ImageJ software was used to measure the particle diameter from the images obtained.

Ultraviolet–visible spectrophotometer (UV-VIS)

In order to confirm loading and calculate encapsulation efficiency, UV-VIS was used to measure the total phenolic content of the electrosprayed BTE-Chitosan nanoparticles. From literature, total phenolic content can be measured at 273 nm. First, a standard curve was made by using known concentrations of BTE dissolved in 90 v/v% acetic acid. Then, BTE-chitosan samples were electrosprayed onto aluminum foil. After spraying onto aluminum foil, the nanoparticles were collected and weighed to determine total chitosan and BTE for each sample. Then, acetone was used to dissolve any free BTE (non-encapsulated) and centrifuged at 16.2 g's for 25 minutes. The acetone-BTE mixture

was then separated from the nanoparticles and the acetone was allowed to fully evaporate in a hood overnight. After evaporation, the BTE residue was dissolved with 90 v/v% acetic acid. It was then run through the UV-VIS machine and absorbance measured at 273 nm. Using the equation from the standard curve, total free BTE was calculated. Total free BTE was then subtracted from the previously calculated total BTE from the dry nanoparticles to determine the amount of BTE that had been encapsulated and the efficiency.

RESULTS & DISCUSSION

The beginning portions of this experiment focused on finding the optimal conditions to achieve the smallest possible particles of chitosan. The parameters tested included the applied voltage, flow rate, chitosan concentration, chitosan molecular weight, and acetic acid concentration.

Voltage and Flow Rate

In an effort to reduce chitosan particle size, electrospray parameters (i.e. voltage and flow rate) were tweaked to see their effects on particle size. Previous research has shown that higher voltage and lower flow rate can reduce chitosan particle sizes during electrospraying (Agnihotri, Mallikarjuna, & Aminabhavi, 2004; Hu, Sheng-Feng, Nair, & Wu, 2012; Huang, Khor, & Lim, 2004). During initial testing of electrospray parameters, 0.6 µL/min flow rate and 15 kV applied voltage were used. However, this flow rate was too low to support a Taylor cone and therefore the cone jet mode of electrospraying was not achieved. Flow rate was increased from 0.6 to 8.33 µL/min and voltage was increased to 20 kV. However, this flow rate was too high for a proper Taylor cone to be made and resulted in the acetic acid not evaporating during the electrospray. The voltage increase was able to stabilize the jet slightly and therefore only flow rate would be changed to find the optimal conditions for a Taylor cone. A reduction of the flow rate to 3µL/min gave mostly stable cone jets resulting in particles being formed for the 330 KDA and 50% acetic acid chitosan particles at a concentration of 5, 10, 20, 30, 50, and 60 mg/ml. These particles can be seen in AFM images in figure 3. From these preliminary AFM images, it was determined that the chitosan particles were larger than expected for nanoparticle

applications. Therefore, it was decided to fine-tune the particle size for reduction by altering chitosan concentration, molecular weight, and acetic acid concentration.

Chitosan Molecular Weight and Acetic Acid Concentration

From previous research, it has been shown that chitosan molecular weight and acetic acid concentration can affect the particle size when electrospraying (Thien, Hsiao, & Ho, 2012). Initially, 330 KDA was used with 50% v/v acetic acid in solutions for electrospraying. However, after initial AFM images of these particles, it was determined that particles were too great in size for nanoparticle applications. In Figure 2, you can see the left image which is 330 KDA chitosan with 50% v/v acetic acid compared to the right image which is the final solution formulation of 130 KDA chitosan with 90% v/v acetic acid. Both of these solutions used 10 mg/ml chitosan. By reducing the molecular weight of chitosan and increasing the acetic acid concentration, drastic particle size reduction was achieved. When the chitosan molecular weight was reduced and the acetic acid concentration was increased, the final flow rate needed to be adjusted to 4 µL/min. This flow rate gave the most stable cone jets as well as the smallest particles for the varying concentrations of chitosan.

Chitosan Concentration

Chitosan concentration also greatly affected the size of the chitosan nanoparticles produced. The AFM images in Figure 3 illustrate this phenomenon. As concentration of chitosan increases from 5 mg/ml to 60 mg/ml, particles increase in size and also increase in aggregation with 60 mg/ml having the largest particles produced. From the preliminary solutions, it was noted that above 50 mg/ml of chitosan in the initial solution created

particles too large so the final concentrations tested were 5, 10, 15, 20, 30 and 40 mg/ml of chitosan.

Preliminary Size and Morphology: AFM

AFM was used to gauge preliminary size and morphology of chitosan and chitosan-BTE nanoparticles after the electrospray parameters and solution properties had been fine tuned. Figure 4 shows the AFM height images of the blank chitosan nanoparticles at varying concentrations (5, 10, 15, 20, 30 and 40 mg/ml). All of these images are 5 μm by 5 μm. These images show that it was possible to achieve spherical particles at all of the concentrations tested. However, at higher concentrations the chitosan nanoparticles seem to slightly deviate from being spherical. It is also apparent that average particle size increases with chitosan concentration, which was an expected result from reading previous research (Thien, Hsiao, & Ho, 2012). Since these AFM images are of height, it is not accurate to measure particle size directly from them. However, it is still possible to see the trend of increasing particle size. The standard deviation of particles can also be seen in these images as some particles appear very small while others are quite large. Figure 5 shows the phase data from the chitosan nanoparticles. From these phase images, more detail of the structures can be seen. An interesting phenomenon that appears in the phase data is strange ‘blobs’ around certain particles. A high amount of them can be seen in the 5 mg/ml chitosan concentration. It is currently unknown what these blobs are from. There has been no previous literature stating such a phenomenon has occurred with chitosan nanoparticles.

Figure 6 shows the AFM height images of chitosan-BTE nanoparticles at varying chitosan concentrations. These images, again, are all 5 µm by 5 µm. These images show that spherical nanoparticles are still obtained at lower concentrations of chitosan with the addition of BTE. At higher concentrations, 30 and 40 mg/ml, the shape of the particles deviate from this. As it was seen in the chitosan blank nanoparticles, increasing chitosan concentration tends to increase the average nanoparticle size. The smallest particles, however, seem to have occurred at the chitosan concentration of 15 mg/ml with the inclusion of BTE. This most likely occurs from the viscosity of the solution being perfect with the electrospray parameters in order to achieve the most stable Taylor cone. The standard deviation of the particle size also increases with increasing chitosan concentration. Figure 7 shows the AFM phase data for the chitosan-BTE nanoparticles. Again, the occurrence of 'blobs' around specific particles occurs in the phase data, which is seen mostly in the 20 mg/ml chitosan-BTE particles. The particles achieved by adding to BTE seem structurally similar to the blank chitosan particles. Unfortunately, it is not possible to confirm loading of BTE into the chitosan with the AFM images.

Based on the information collected from these AFM images, it was decided to continue on to SEM with the current chitosan and chitosan-BTE nanoparticles in order to see more detailed morphology and also accurately measure the sizes of the particles.

Size and Morphology: SEM

Figure 8 contains SEM images of all the chitosan blank nanoparticles. It can be seen in the 5 mg/ml image (top left) that extremely small particles can be achieved. However, some of these particles appear to be irregularly shaped which indicates that the

Taylor jet cone was not as stable as it could be. It can be seen that as chitosan concentration increases to 10 and 15 mg/ml, particles become much more uniform in size and shape. This indicates that the electrospray parameters used are best suited for these two concentrations for the blank chitosan nanoparticles. As the chitosan concentration increases beyond 15 mg/ml, there are a few things that begin to happen. One, the shape of the particles starts to again become irregular as was seen in the lowest chitosan concentration. Two, the standard deviation increases drastically with very large particles being present along with very small particles. Three, at the highest concentrations it is possible to see 'lines' that are connecting particles together. These are fibers that are being formed which mean that at these higher concentrations, electrospinning begins to occur. Electrospinning is a similar process to electrospraying, however instead of forming particles, fibers and mats are formed. This phenomenon tends to occur with higher viscosity samples. Therefore, the most likely reason this only occurs at the higher concentrations of chitosan is the drastic increase in viscosity of the samples.

Figure 9 contains SEM images of all the chitosan-BTE nanoparticles. By comparing these images to the blank chitosan images in figure 8, it is possible to see that the inclusion of BTE did not seem to affect the two lowest concentrations of chitosan (5 and 10 mg/ml). However, above these concentrations, the addition of BTE seemed to greatly affect the particles that were formed. The standard deviation of the higher chitosan concentrations greatly increased. Also, the increase in particle size from increasing chitosan concentration seems to have shifted with the BTE inclusion. The smallest particles formed seem to be from 20 mg/ml chitosan with BTE. However, these particles are irregularly shaped which is not optimal for the electrospraying process. In

the larger concentrations of chitosan, again it is possible to see fibers being formed which means the high viscosity of the solution is producing an electrospinning effect instead of electrospraying.

SEM images allow the possibility to accurately measure particle size of all chitosan and chitosan-BTE nanoparticles. First, the one micrometer scale was imported into a program called ImageJ. With the scale imported, it is then possible to hand measure the particles diameter to determine their size. For each image, 100 particles were randomly selected to be measured.

Figures 11 – 16 are histograms for each of the chitosan blank nanoparticles that were created from measuring particle sizes. Table 1 has the means and standard deviations calculated for the nanoparticles as well. From table 1, it is possible to see that in general, the mean increases as chitosan concentration increases. However, the largest average particle size is not the highest chitosan concentration. A better indication of the increasing particle size would actually be the standard deviation which increases as chitosan concentration increases. The average particle size is skewed from extremely large particle and extremely tiny particles, which can be seen in the histograms from figures 11-16. Therefore it is important to look at the standard deviation calculated. From these histograms and table, it is possible to see the increase in standard deviation with increasing chitosan concentration which is what was seen from AFM and SEM images. In the smaller concentrations, such as 5 mg/ml chitosan blank in figure 11, the standard deviation is much smaller and the particle size is evenly distributed around a central size which in this case is 300-400 nm. From table 1, you can see that it has the smallest standard deviation of the chitosan nanoparticles and also the smallest mean particle size.

As chitosan concentration is increased in the chitosan blank particles, the standard deviation greatly increases. In figure 14, it can be seen that the 30 mg/ml chitosan blank particles are not centralized around a specific peak and instead are spread out across the entire histogram. From table 1 you can see that the standard deviation is quite high at 294.52 nm.

Figures 17-21 provide histograms of chitosan-BTE nanoparticle sizes from varying chitosan concentrations. In table 2, the data from these histograms is quantified as averages and standard deviations of the chitosan-BTE nanoparticles. Again, as chitosan concentration increases, the mean particle diameter and standard deviation tend to increase. However, at 20 and 30 mg/ml, standard deviation was actually reduced. Therefore the addition of the BTE seems to be reducing standard deviation of particle diameter at higher concentrations of BTE. But as previously discussed, and shown in figure 9, these particles are irregularly shaped and not entirely suited for use.

While SEM provided valuable morphology information and accurate particle size, it was unclear if the BTE had been successfully loaded into the chitosan-BTE nanoparticles. In order to gain this information, the chitosan-BTE nanoparticles were subjected to UV-VIS to measure encapsulation efficiency.

Encapsulation Efficiency

Encapsulation efficiency of the BTE-Chitosan nanoparticles was determined by UV-VIS. In order to measure how much BTE was loaded into the chitosan nanoparticles, a standard curve of known BTE concentrations was first made, which can be seen in figure 22. This curve gave us the equation $y = 33.964x + 0.0141$ where x is the

concentration of BTE and y is the absorbance measured at 273 nm. Table 3 has the efficiencies for all the chitosan-BTE particles tested. All particles, except the 40 mg/ml chitosan-BTE particles, had greater than 95% encapsulation efficiency. Based on previous research, this is on the highest end of encapsulation efficiency recorded from electrospraying (Gomez-Estaca, Balaguer, Gavara, & Hernandez-Munoz, 2012). This is extremely efficient encapsulation and a much greater value than other encapsulation methods. The highest concentration of chitosan (40 mg/ml) and BTE nanoparticles only had 76.8% efficiency but this is still quite high. The lower efficiency could be due to the electrospinning effect where fibers are formed instead of particles. With less particles formed and fibers forming instead, the encapsulation efficiency could decrease.

CONCLUSION

Fine-tuning chitosan nanoparticle size via electrospray parameters

The first part of this study focused on tuning chitosan nanoparticles by adjusting the electrospraying parameters. One of the main parameters to be adjusted is flow rate. To create the smallest particles, it was found that flow rate needs to be tuned so that it is fast enough to create a stable Taylor cone but also slow enough that the solvent has sufficient time to evaporate as it travels toward the collector. This was seen in testing during initial chitosan nanoparticle creation as a 0.6 µL/min flow rate was too slow for a Taylor cone jet but when increased to 8.33 µL/min was too fast to achieve the desired nanoparticle size. After adjustments to chitosan KDA, a final flow rate of 4 µL/min was used and this created the best chitosan nanoparticles with a stable Taylor cone. In general, increasing flow rate increased particle size after finding the correct Taylor cone flow rate.

Voltage is also an important parameter when tuning particle size of electrospraying. During initial testing of chitosan nanoparticles, 15 kV was used in the electrospray procedure. It was found that by increasing this voltage to 20 kV a more stable Taylor cone was produced which resulted in creating smaller chitosan nanoparticles. In general, it was found that increasing voltage decreased average particle size due to the additional stabilization.

Fine-tuning chitosan nanoparticle size via solution properties

In addition to using electrospray parameters, particle size can also be fine-tuned by changing the initial solution properties. The main two solution properties to be adjusted were chitosan concentration and acetic acid concentration. From results it was

seen that in general, increasing chitosan concentration of the solution also increased the average particle size. There were some exceptions to this in the results found and is probably due to creating a more stable Taylor cone due to the viscosity of the solution at specific chitosan concentrations. Acetic acid concentration also changed the nanoparticle size created. Increasing the acetic acid concentration decreased the average nanoparticle size of the chitosan.

Greater Encapsulation Efficiency

Encapsulation efficiency is an important final parameter of nanoparticle production. High encapsulation efficiency results in more particles being created correctly and less waste of active compounds, in this case BTE. In this study, over 95% encapsulation efficiency was achieved in all but one case. This efficiency matches previous literature on electrospraying where it was found to have 80-96% encapsulation efficiency (Ding, Lee, & Wang, 2005; Xie, Marijnissen, & Wang, 2006). Other methods of nanoparticle production fail to achieve encapsulation efficiency this high. In a supramolecular self-organizing reaction of chitosan, lecithin, and quercetin, encapsulation efficiency was only able to reach 45-51% (Tan, Liu, Guo, & Zhai, 2011).

Nanoparticle Creation in a One-Step Process

A major objective of this study was to create nanoparticles in a one step process. In other pathways of nanoparticle creation, often multiple steps are needed after the particles have formed to remove the solvent they are in. This can be time consuming and tedious to achieve. By using electrospraying, it is possible to go from a solution containing all the pieces of the desired nanoparticle directly to a dry powdered finished

product. By using a one step process, the time to create nanoparticles is greatly diminished compared to other methods that need to remove a solvent from the created nanoparticles. The entire production process of electrospraying is also much simpler. After calculations and testing of parameters, the procedure is straight forward and can be taught to someone in a production facility that does not have the background in the chemical and physical properties of electrospraying, which can be beneficial to scaling this procedure up to industrial standards.

FUTURE WORK AND APPLICATIONS

MTT Assay

In order to more fully understand the particle created, future studies will be needed to see how the BTE-chitosan nanoparticles react *in vitro* and *in vivo*. The first experiment for future work would be an MTT assay on HepG2 to see how our particle can reduce the cancer cell viability. Preliminary data has been collected for this MTT assay as controls have been tested on HepG2 cancer cells. The first step of the MTT assay was to test the pure BTE on HepG2 cells. The graph of cell viability versus pure BTE can be seen in figure 23. From this figure it is possible to see that BTE did not have a significant reduction in cell viability until the BTE concentration reached 100 µg/ml. At this concentration, the cell viability was reduced to ~72%. When the pure BTE concentration was increased to 200 µg/ml, the cell viability drastically reduced to ~17%.

The next step was to test the chitosan nanoparticle vehicle without the BTE. This was to test to see if the chitosan vehicle had any effect on the HepG2 cells. Figure 24 has a graph of cell viability with differing concentrations of the chitosan blank nanoparticle. From this graph it can be seen that the chitosan nanoparticle has no effect on the HepG2 cell viability. Having the vehicle be inert to the cells is a control to show that when the chitosan-BTE nanoparticles are used to treat the cells, it will show that the reduction in cell viability is from the active compound and not the vehicle itself.

The final step for this MTT assay data will be to run the assay on the BTE-chitosan particles itself. Currently, the hypothesis is the particles will reduce the viability of the cancer cells with a smaller concentration of BTE than the pure BTE will.

Cellular Uptake

After finishing the MTT assay, a cellular uptake study will also be performed. In order to use the fluorescent microscope to perform the cell uptake study, the chitosan used needs to be labeled with a fluorescent compound. Fluorescein isothiocyanate (FTIC) can be used to label chitosan. This step has been completely and an FTIC labeled chitosan. The procedures for labeling chitosan with FTIC was done as described by Hu et al. 2012, which is as follows and slightly modified to increase the amount of the final product. Dehydrated methanol (100 ml) and FTIC (50 ml, 20mg/ml in methanol) was added to chitosan (100 ml, 1% in 0.1M acetic acid). This was done in a dark room at ambient temperature and left for three (3) hours. After three hours, the FTIC labeled chitosan was percipitated out using 0.2 M NaOH. Then pelleting was done at 40,000 x g for 10 minutes then washed with methanol:water (70:30 v/v). The labeled chitosan was then redissolved in 20 ml of 0.1 M acetic acid. This was then dialyzed in the dark against 5 L of water for one week with water being changed every 24 hours. After, the FTIC-labaled chitosan was freeze dried. This FTIC labeled chitosan can now be used in the creation of BTE-chitosan nanoparticles as described in the methods section of this paper. This new particle can be observed with a florescent microscope to observe cellular uptake.

Fourier Transform Infrared Spectroscopy (FTIR)

Currently it is unknown if chitosan has bonding effects with the BTE used to create these nanoparticles. If this BTE has binding effects, then the procedure to measure encapsulation efficiency would need to be changed as acetone would have a difficult time

washing the free BTE off the particles as described in the methods of encapsulation efficiency. In order to see this, chitosan and BTE need to be observed in a FTIR to see if there is a band shift. If there is a band shift when this procedure is formed, then there is hydrogen bonding occurring between BTE and chitosan.

Application

This chitosan-BTE nanoparticle can potentially be used as a food additive in a product such as a sport drink. The BTE has been shown to benefit muscle recovery after workouts (Arent, Senso, Golem, & McKeever, 2010). However, there needs to be more testing before human consumption to ensure safety. Future work to ensure proper safety includes more *in vitro* testing as well was *in vivo* testing on models such as mice. Following good results from these studies, approval can be achieved to be used as a food additive.

BIBLIOGRAPHY

Agnihotri, S., Mallikarjuna, N., & Aminabhavi, T. (2004). Recent advances on chitosan-based micro- and nanoparticles in drug delivery. *Journal of Controlled Release , 100* (1), 5-28.

Aneja, R., Odoms, K., Denenberg, A., & Wong, H. (2004). Theaflavin, a black tea extract, is a novel anti-inflammatory compound. *Critical Care Medicine , 32* (10), 2097-2103.

Arent, S., Senso, M., Golem, D., & McKeever, K. (2010). The effects of theaflavin-enriched black tea extract on muscle soreness, oxidative stress, inflammation, and endocrine responses to acute anaeerobic interval training: a randomized, double-blind, crossover study. *Journal of the International Soceity of Sports Nutrition , 7* (11), 1-10.

Damodaran, S., Parkin, K. L., & Fennema, O. R. (2008). *Fennema's Food Chemistry.* CRC Press.

Ding, L., Lee, T., & Wang, C. (2005). Fabrication of monodispersed taxol-loaded particles using electrohydrodynamic atomization. *Journal of Controlled Release , 102* (2), 395-413.

Dodane, V., & Vilivalam, V. (1998). Pharmaceutical applications of chitosan. *Pharmacetuical Science & Technology Today , 1* (6), 246-253.

Gomez-Estaca, J., Balaguer, M., Gavara, R., & Hernandez-Munoz, P. (2012). Formation of zein nanoparticles by electrohydrodynamic atomization: Effect of the main processing variables and suitability for encapsulating the food color and active ingredient curcumin. *Food Hydrocolloids , 28* (1), 82-91.

Gosslau, A., Jao, D. L., Huang, M.-T., Ho, C.-T., Evans, D., Rawson, N., et al. (2011). Effects of the black tea polyphenol theaflavin-2 on apoptotic and inflammatory pathways in vitro and in vivo. *Molecular Nutrition & Food Research , 55*, 198-208.

Gosslau, A., Li En Jao, D., Huang, M.-T., Ho, C.-T., Evans, D., Rawson, N. E., et al. (2011). Effects of the black tea polyphenol theaflavin-2 on apoptotic and inflammatory pathwaysin vitro and in vivo. *Molecular Nutrition and Food Research , 55*, 198-208.

Hu, B., Ting, Y., Zeng, X., & Huang, Q. (2012). Cellular uptake and cytotoxicity of chitosan-caseinophosphopeptides nanocomplexes loaded with epigallocatechin gallate. *Carbohydrate Polymers , 89*, 362-370.

Hu, J., Sheng-Feng, L., Nair, G., & Wu, W. (2012). Predicting chitosan particle size produced by electrohydrodynamic atomization. *Chemical Engineering Sciences , 82*, 159-165.

Huang, M., Khor, E., & Lim, L.-Y. (2004). Uptake and Cytotoxicity of Chitosan Molecules and Nanoparticles: Effects of Molecular Weight and Degree of Deacetylation. *Pharmaceutical Research , 21* (2), 344-353.

Huang, Q. (2012). *Nanotechnology in the food, beverage and nutraceutical industry.* Woodhead Publishing Limited.

Jaworek, A. (2007). Micro- and nanoparticle production by electrospraying. *Powder Technology , 176*, 18-35.

Jaworek, A., & Krupa, A. (1999). Classification of the modes of EHD spraying. *Journal of Aerosol Science , 30*, 873-893.

Jaworek, A., & Sobcyzk, A. (2008). Electrospraying route to nanotechnology: An overview. *Journal of Electrostatics , 66*, 197-219.

Jung, J. H., Park, S. Y., Lee, J. E., Nho, C. W., Lee, B. U., & Bae, G. N. (2011). Electrohydrodynamic nano-spraying of ethanolic natural plant extracts. *Journal of Aerosol Science , 42*, 725-736.

Kuhnert, N. (2010). Unraveling the structure of the black tea thearubigins. *Archives of Biochemistry and Biophysics , 501*, 37-51.

Laelorspoen, N., Wongsasulak, S., Yoovidhya, T., & Devahastin, S. (2014). Microencapsulation of Lactobacillus acidophilus in zein–alginate core–shell microcapsules via electrospraying. *Journal of Functional Foods , 7*, 342-349.

Lee, Y.-H., Bai, M.-Y., & Chen, D.-R. (2011). Multidrug Encapsulation by Coaxial Tri-Capillary Electrospray. *Colloids and Surfaces B: Biointerfaces , 82*, 104-110.

Luczaj, W., & Skrzydlewska, E. (2005). Antioxidative Properties of Black Tea. *Preventive Medicine , 40*, 910-918.

Salata, O. (2005). Tools of Nanotechnology: Electrospray. *Current Nanoscience , 1*, 25-33.

Tan, Q., Liu, W., Guo, C., & Zhai, G. (2011). Preparation and evaluation of quercetin-loaded lecithin-chitosan nanoparticles for topical delivery. *International Journal of Nanomedicine , 6*, 1621-1630.

Thien, D. V., Hsiao, S. W., & Ho, M. H. (2012). Synthesis of Electrosprayed Chitosan Nanoparticles for Drug Sustained Release. *Nano LIFE , 2* (1), 125003-1-125003-11.

Vani, R., & Shaleesha, S. (2013). Studies on the extraction of chitin and chitosan from different aquatic organisms. *Advanced Biotechnology , 12* (12), 12-15.

Xie, J., Marijnissen, J., & Wang, C. (2006). Microparticles developed by electrohydrodynamic atomization for the local delivery of anticancer drug to treat C6 glioma in vitro. *Biomaterials , 27* (17), 3321-3332.

Xie, J., Ng, W. J., Lee, L. Y., & Wang, C.-H. (2008). Encapsulation of Protein Drugs in Biodegradable Microparticles by Co-Axial Electrospray. *Journal of Colloid and Interface Sciences , 317*, 469-476.

Yu, D., Wang, X., Lu, P., Chen, X., Zhao, H., Li, X., et al. (2012). Colon-Targeted Drug Delivery Microparticles Prepared Using Electrohydrodynamic Atomization. *Applied Mechanics and Materials , 130-134*, 1663-1667.

Zhang, S., & Kawakami, K. (2010). One-step preparation of chitosan solid nanoparticles by electrospray deposition. *International Journal of Pharmaceutics , 397*, 211-217.

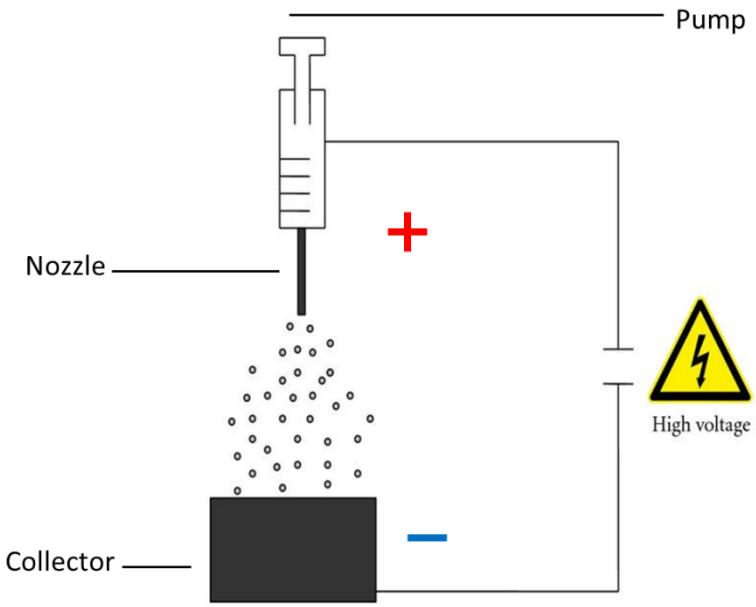

Figure 1. A basic diagram of an electrospraying setup which consists of a high voltage power supply, a pump attached to a syringe, and a grounded collector where the finished nanoparticles

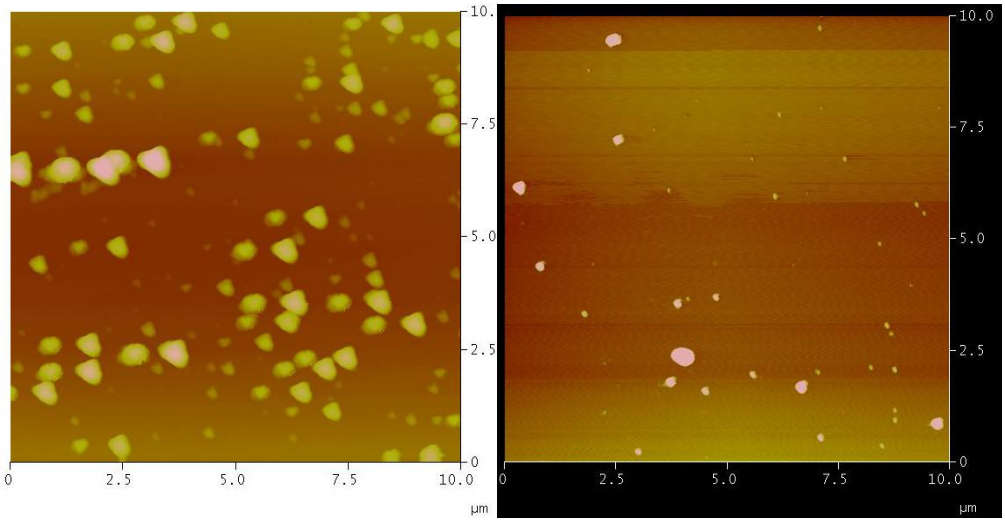

Figure 2. The left picture is an AFM of Chitosan particles made with 330 KDA Chitosan and 50% v/v Acetic Acid. The right picture is an AFM of Chitosan particles made with 130 KDA Chitosan and 90% v/v Acetic Acid. With a higher KDA of chitosan and a lower acetic acid concentration, particles are much larger than in the final formulation.

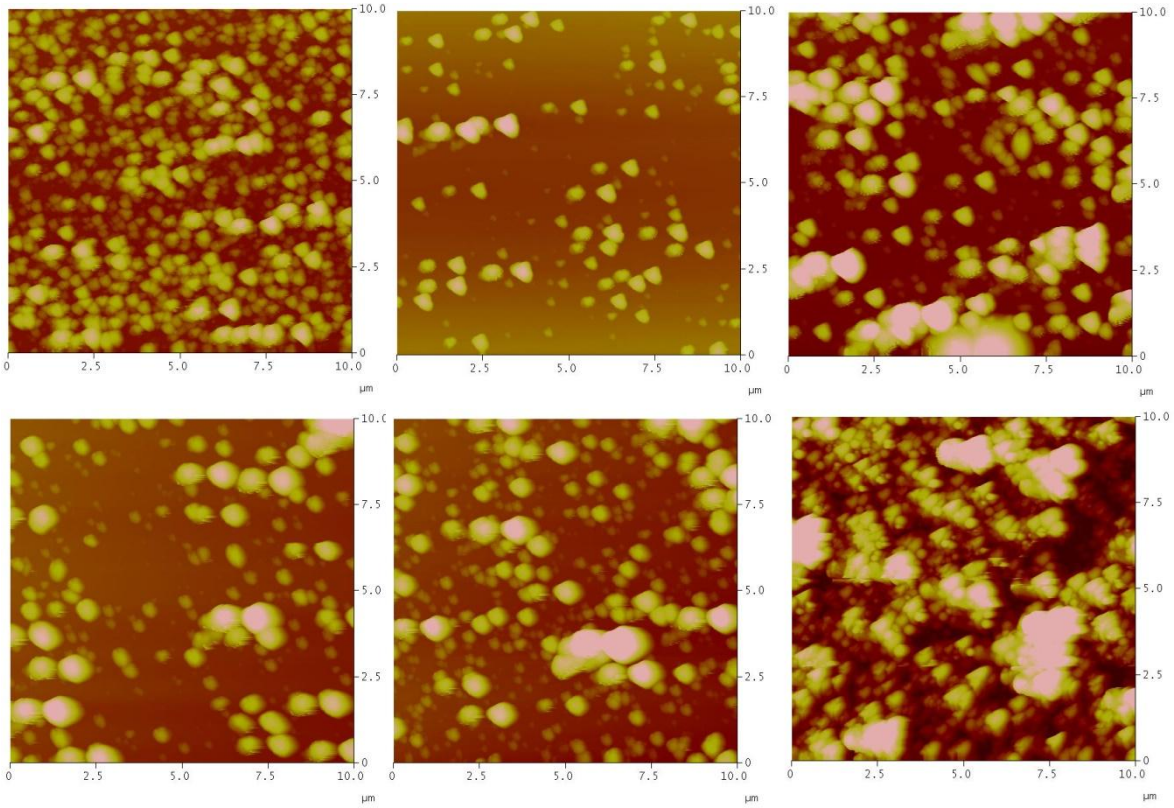

Figure 3. AFM height images of chitosan concentrations at 5 mg/ml (top left), 10 mg/ml (top middle), 20 mg/ml (top right), 30 mg/ml (bottom left), 50 mg/ml (bottom middle), and 60 mg/ml (bottom right) of 330 KDA Chitosan with 50% v/v acetic acid. Electrospray parameters were 20 kV applied voltage, 3 µL/min, 10cm working distance, and 2 minute spray intervals.

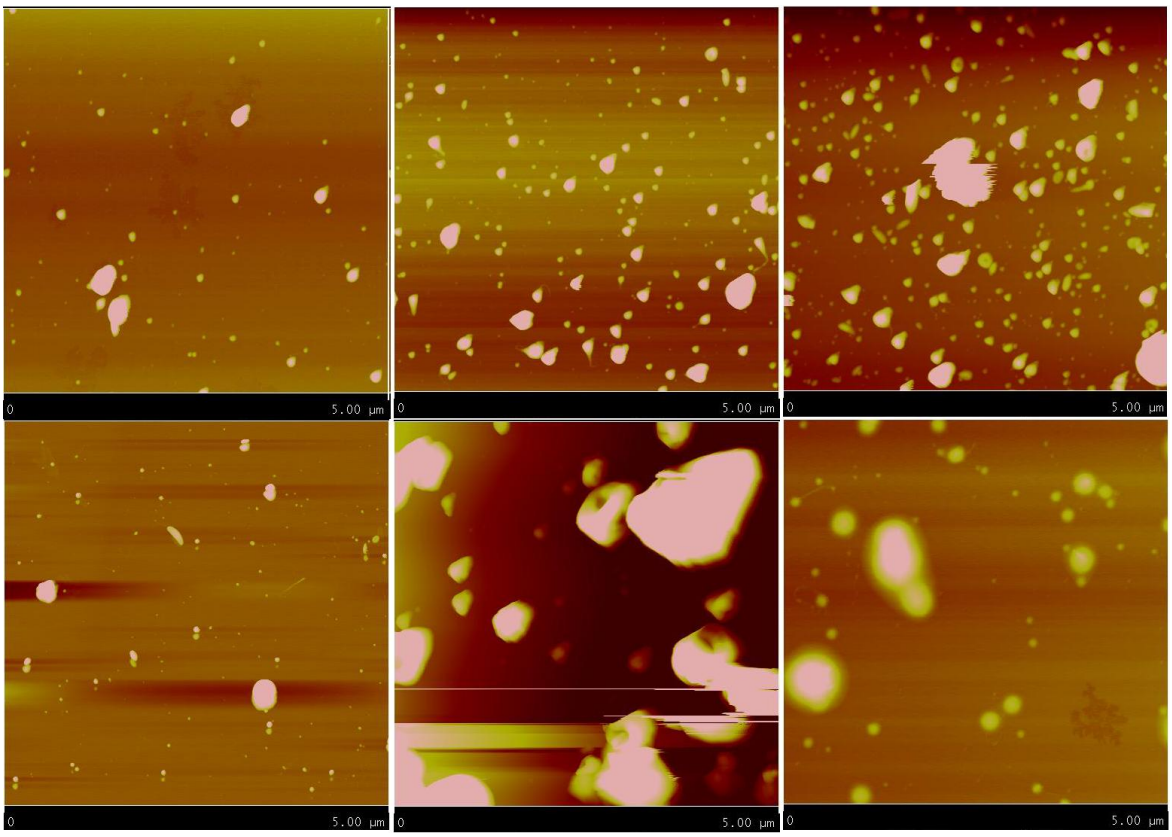

Figure 4. AFM height images of chitosan concentrations at 5 mg/ml (top left), 10 mg/ml (top middle), 15 mg/ml (top right), 20 mg/ml (bottom left), 30 mg/ml (bottom middle), and 40 mg/ml (bottom right) of 130 KDA Chitosan with 90% v/v acetic acid. Electrospray parameters were 20 kV applied voltage, 4 µL/min, 10cm working distance, and 5 minute spray intervals. All images are 5 µm by 5 µm.

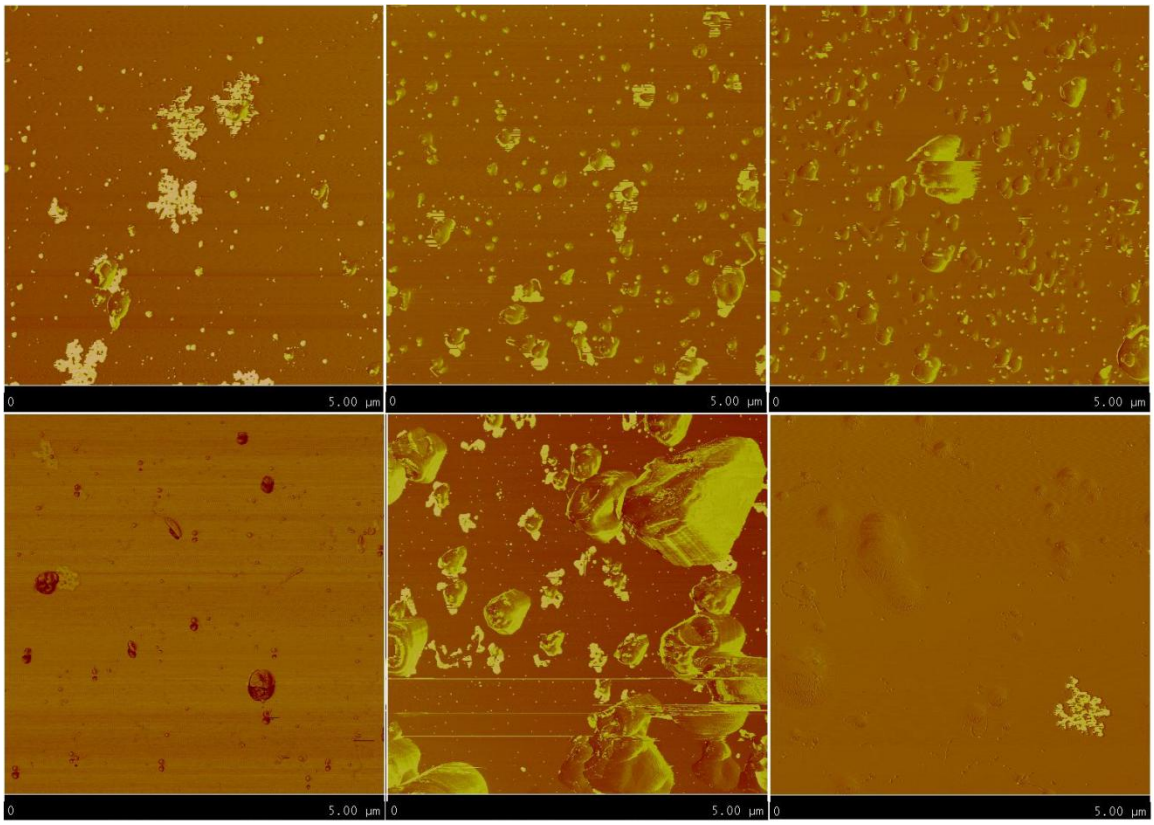

Figure 5 AFM phase images of chitosan concentrations at 5 mg/ml (top left), 10 mg/ml (top middle), 15 mg/ml (top right), 20 mg/ml (bottom left), 30 mg/ml (bottom middle), and 40 mg/ml (bottom right) of 130 KDA Chitosan with 90% v/v acetic acid. Electrospray parameters were 20 kV applied voltage, 4 µL/min, 10cm working distance, and 5 minute spray intervals. All images are 5 µm by 5 µm.

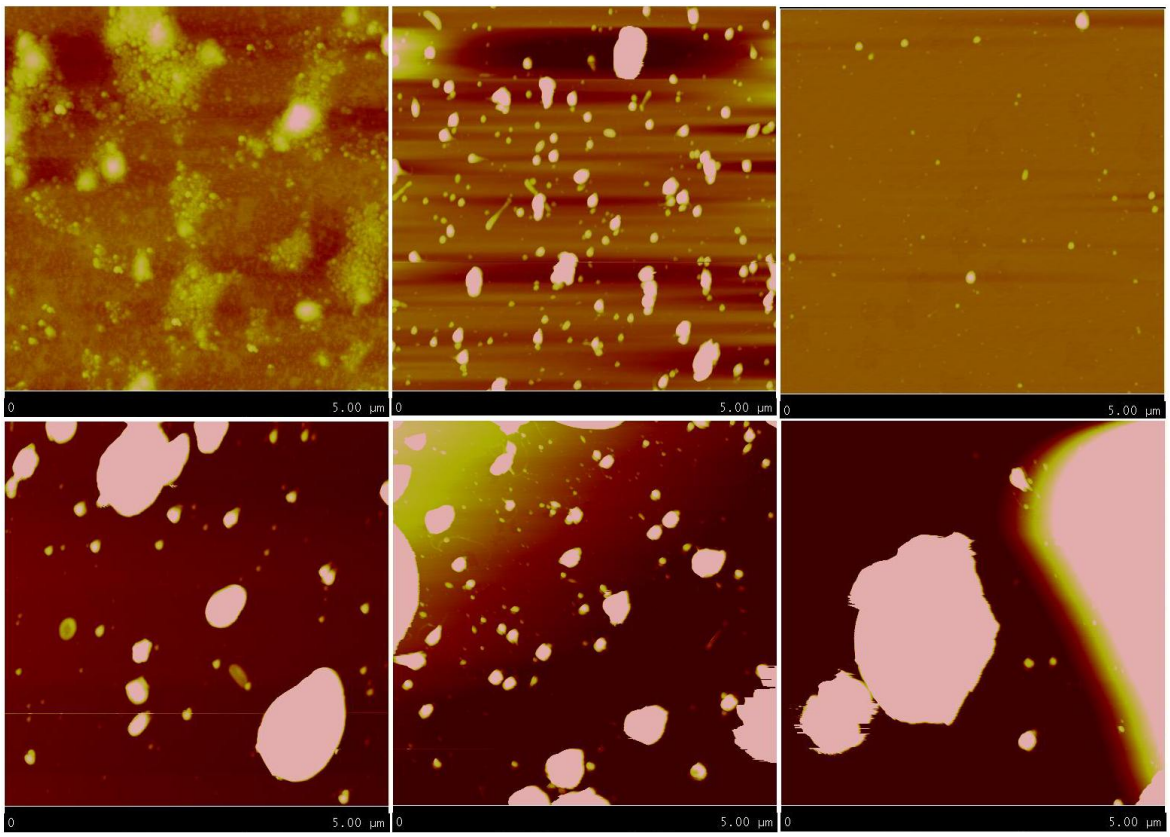

Figure 6. AFM height images of chitosan-BTE particles. All particles used a concentration of 1 mg/ml BTE. Chitosan concentrations at 5 mg/ml (top left), 10 mg/ml (top middle), 15 mg/ml (top right), 20 mg/ml (bottom left), 30 mg/ml (bottom middle), and 40 mg/ml (bottom right) of 130 KDA Chitosan with 90% v/v acetic acid. Electrospray parameters were 20 kV applied voltage, 4 µL/min, 10cm working distance, and 5 minute spray intervals. All images are 5 µm by 5 µm.

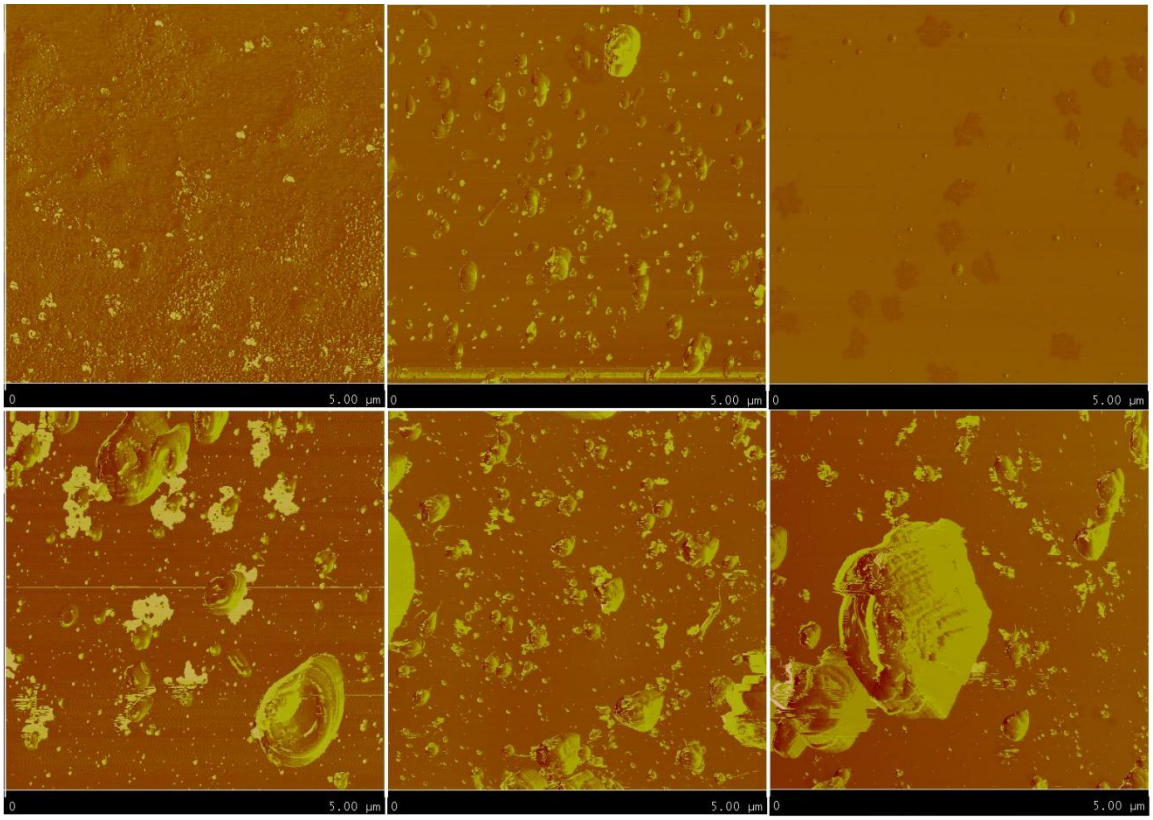

Figure 7. AFM phase images of chitosan-BTE particles. All particles used a concentration of 1 mg/ml BTE. Chitosan concentrations at 5 mg/ml (top left), 10 mg/ml (top middle), 15 mg/ml (top right), 20 mg/ml (bottom left), 30 mg/ml (bottom middle), and 40 mg/ml (bottom right) of 130 KDA Chitosan with 90% v/v acetic acid. Electrospray parameters were 20 kV applied voltage, 4 µL/min, 10cm working distance, and 5 minute spray intervals. All images are 5 µm by 5 µm.

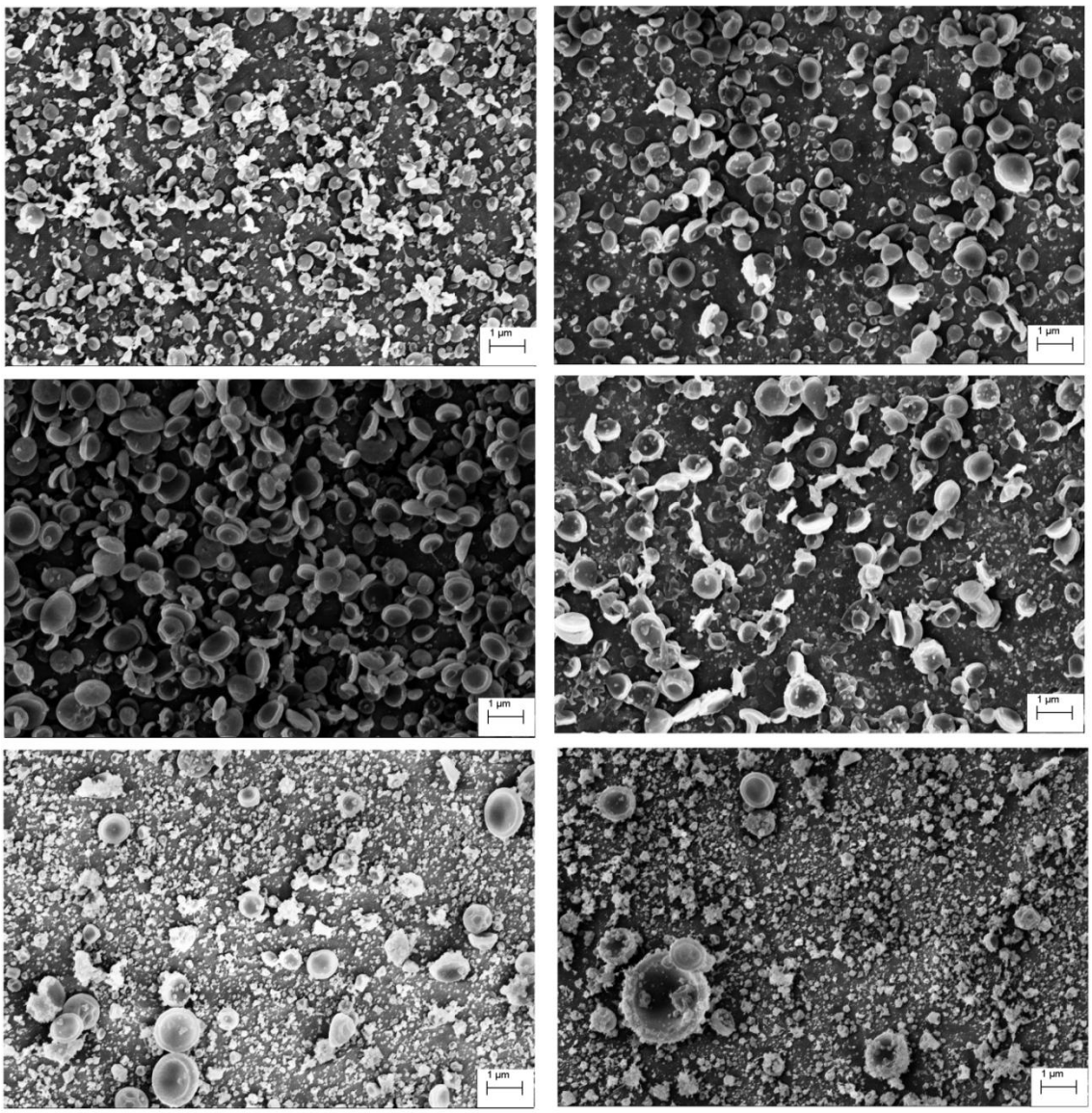

Figure 8. SEM images of chitosan blank particles. Initial solution concentrations are 5 mg/ml (top left), 10 mg/ml (top right), 15 mg/ml (middle left), 20 mg/ml (middle right), 30 mg/ml (bottom left), 40 mg/ml (bottom right).

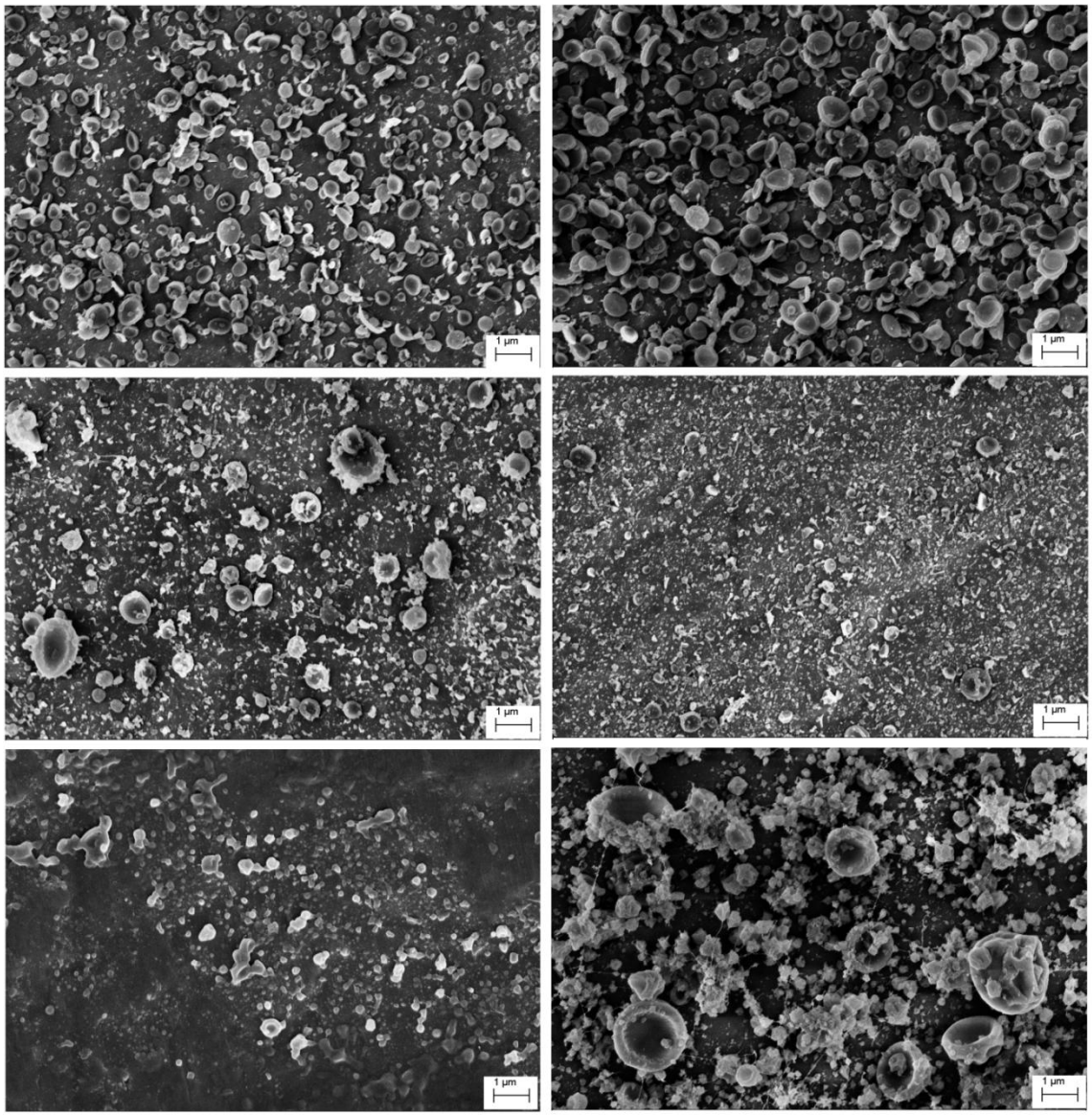

Figure 9. SEM images of chitosan-BTE particles. Initial solution concentrations are 5 mg/ml (top left), 10 mg/ml (top right), 15 mg/ml (middle left), 20 mg/ml (middle right), 30 mg/ml (bottom left); 40 mg/ml (bottom right).

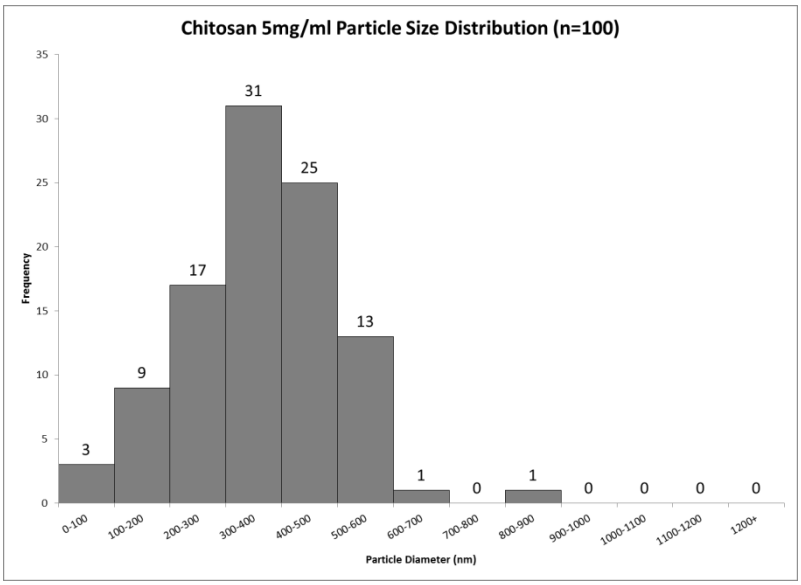

Figure 10. Histogram of 5 mg/ml chitosan nanoparticle size distribution. Sizes were measured in ImageJ with a sample population of 100.

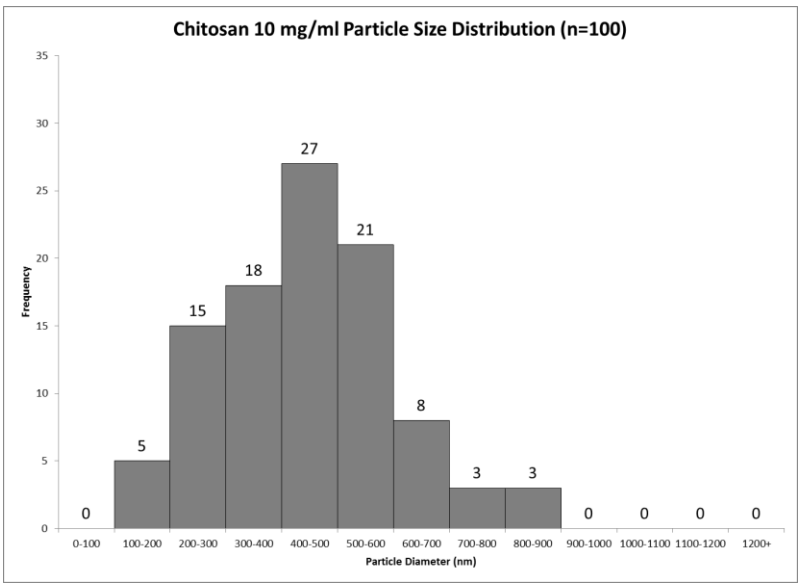

Figure 11. Histogram of 10 mg/ml chitosan nanoparticle size distribution. Sizes were measured in ImageJ with a sample population of 100.

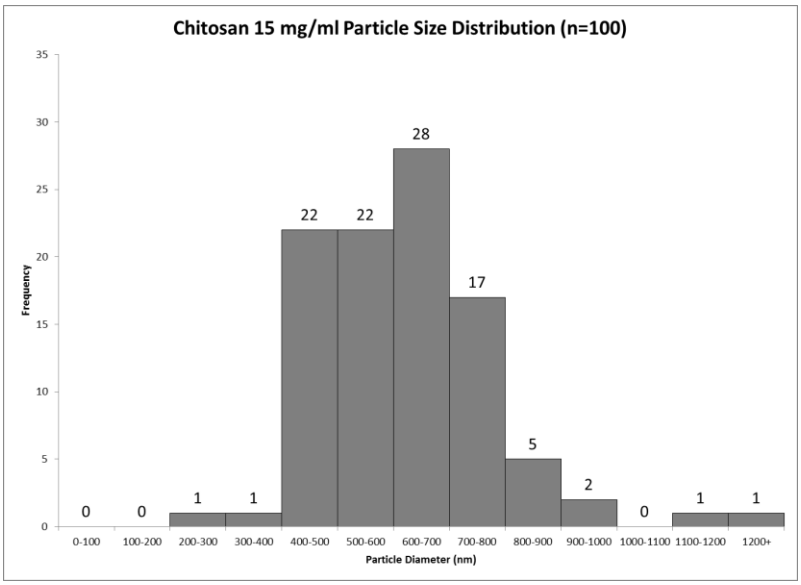

Figure 12. Histogram of 15 mg/ml chitosan nanoparticle size distribution. Sizes were measured in ImageJ with a sample population of 100.

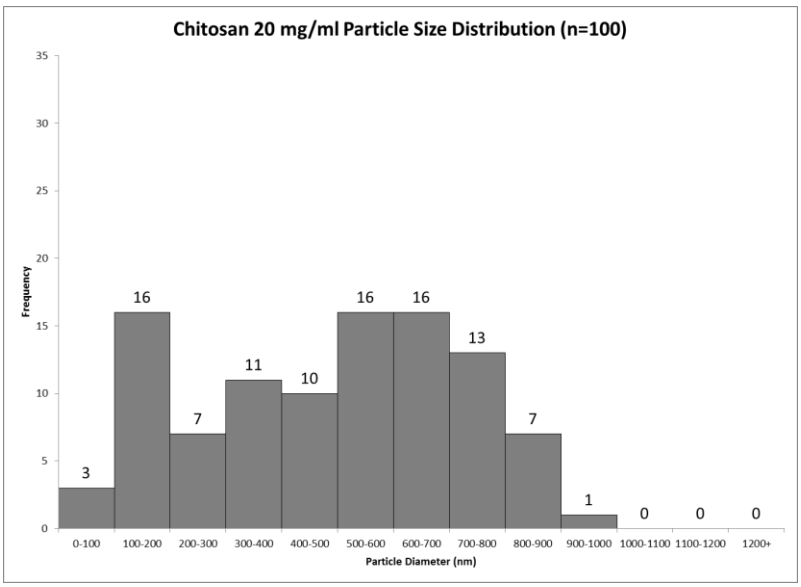

Figure 13. Histogram of 20 mg/ml chitosan nanoparticle size distribution. Sizes were measured in ImageJ with a sample population of 100.

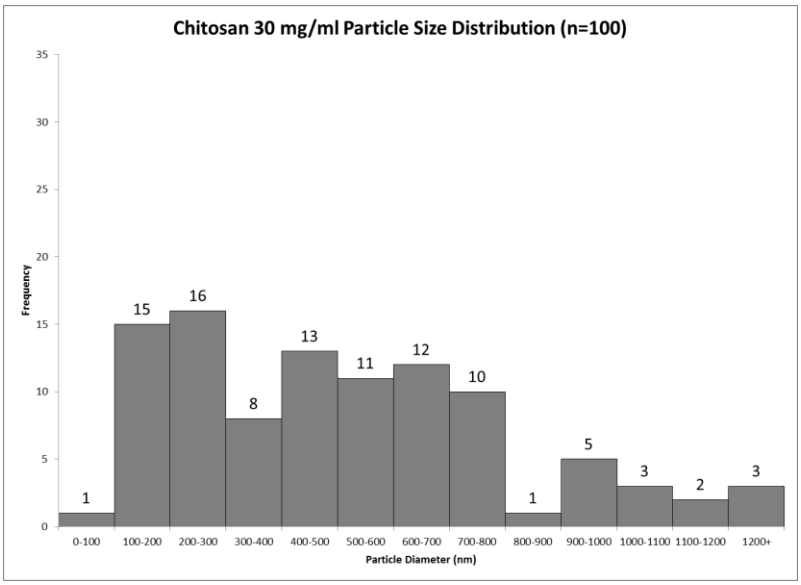

Figure 14. Histogram of 30 mg/ml chitosan nanoparticle size distribution. Sizes were measured in ImageJ with a sample population of 100.

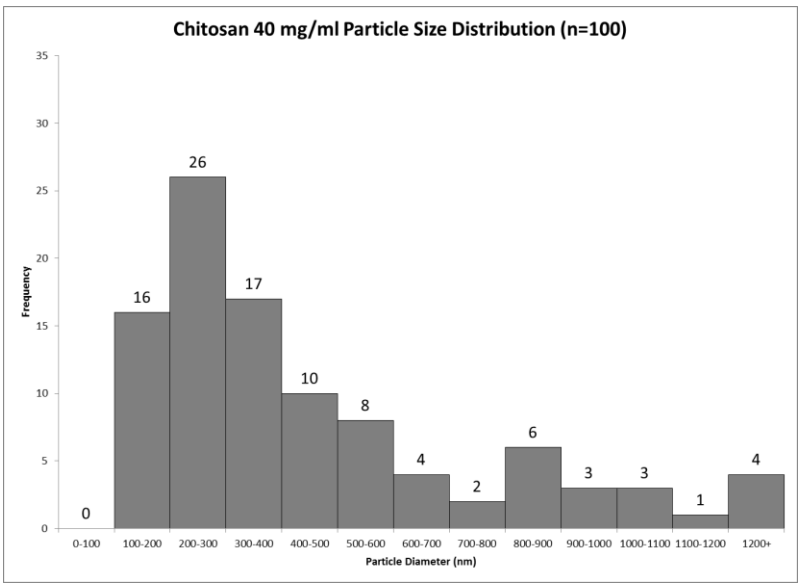

Figure 15. Histogram of 40 mg/ml chitosan nanoparticle size distribution. Sizes were measured in ImageJ with a sample population of 100.

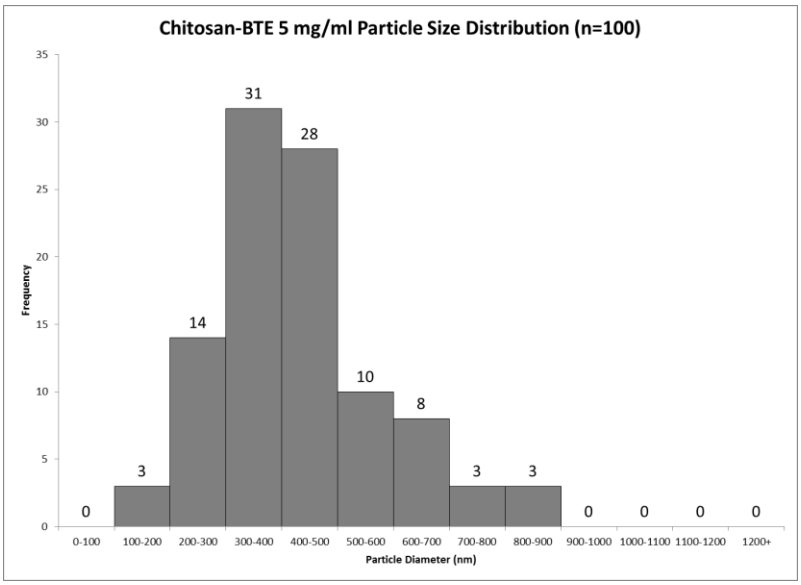

Figure 16. Histogram of 5 mg/ml chitosan-BTE nanoparticle size distribution. Sizes were measured in ImageJ with a sample population of 100.

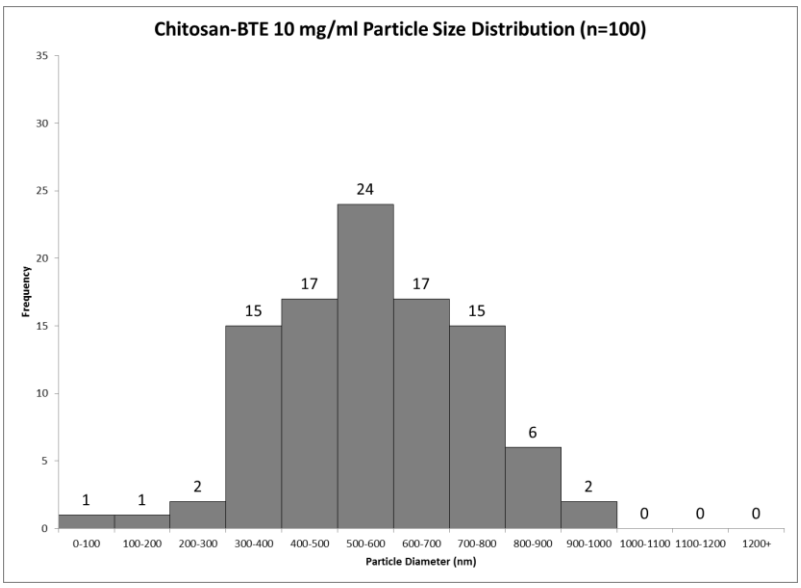

Figure 17. Histogram of 10 mg/ml chitosan nanoparticle size distribution. Sizes were measured in ImageJ with a sample population of 100.

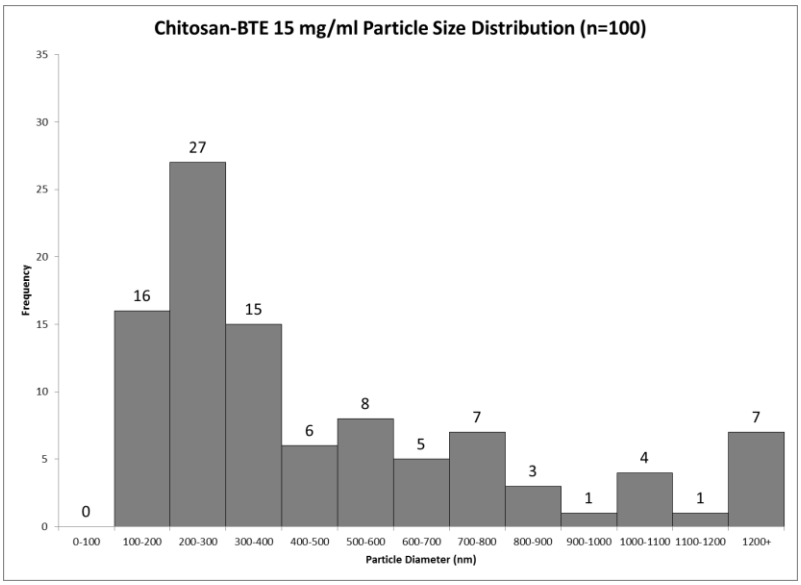

Figure 18. Histogram of 15 mg/ml chitosan nanoparticle size distribution. Sizes were measured in ImageJ with a sample population of 100.

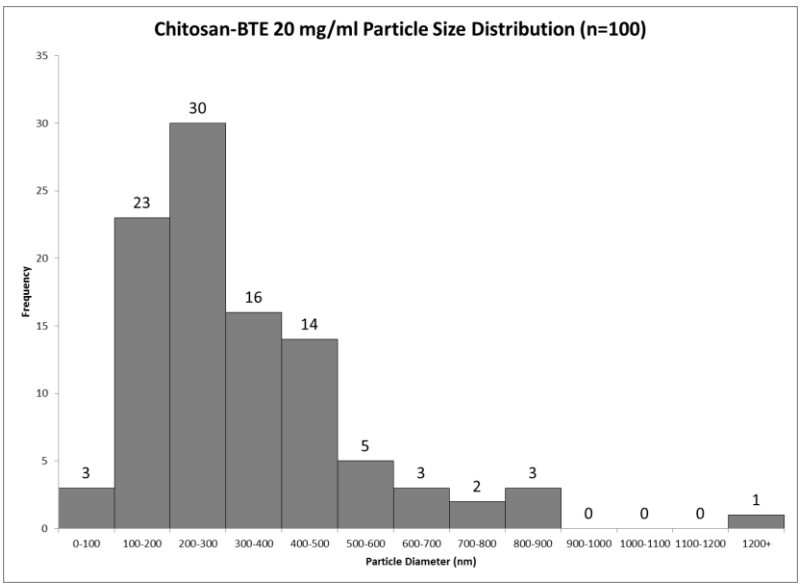

Figure 19. Histogram of 20 mg/ml chitosan nanoparticle size distribution. Sizes were measured in ImageJ with a sample population of 100.

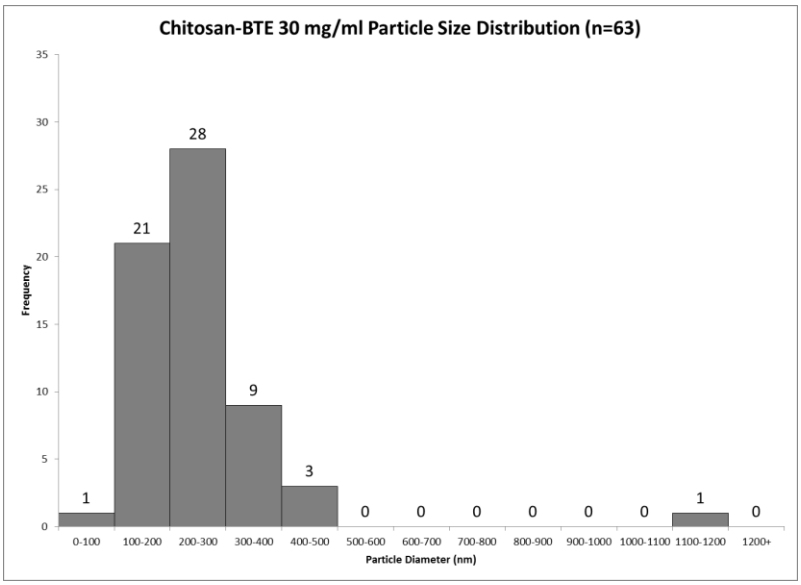

Figure 20. Histogram of 30 mg/ml chitosan nanoparticle size distribution. Sizes were measured in ImageJ with a sample population of 100.

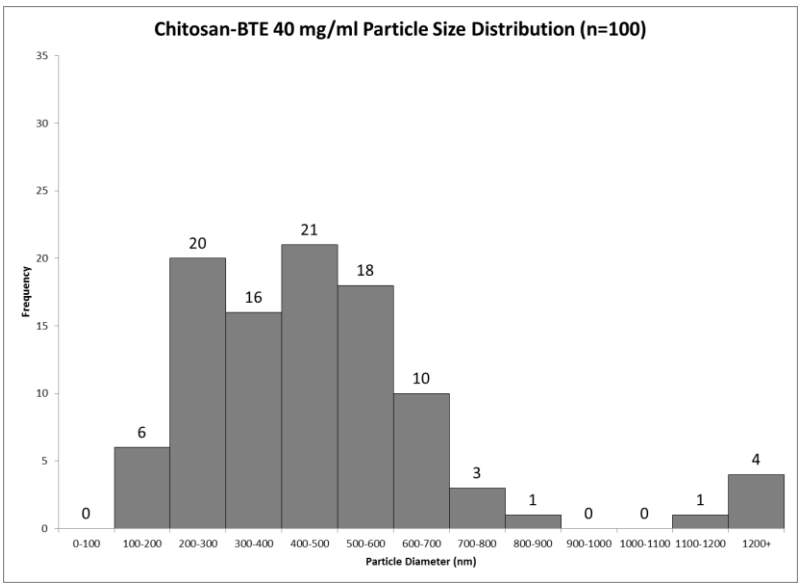

Figure 21. Histogram of 40 mg/ml chitosan nanoparticle size distribution. Sizes were measured in ImageJ with a sample population of 100.

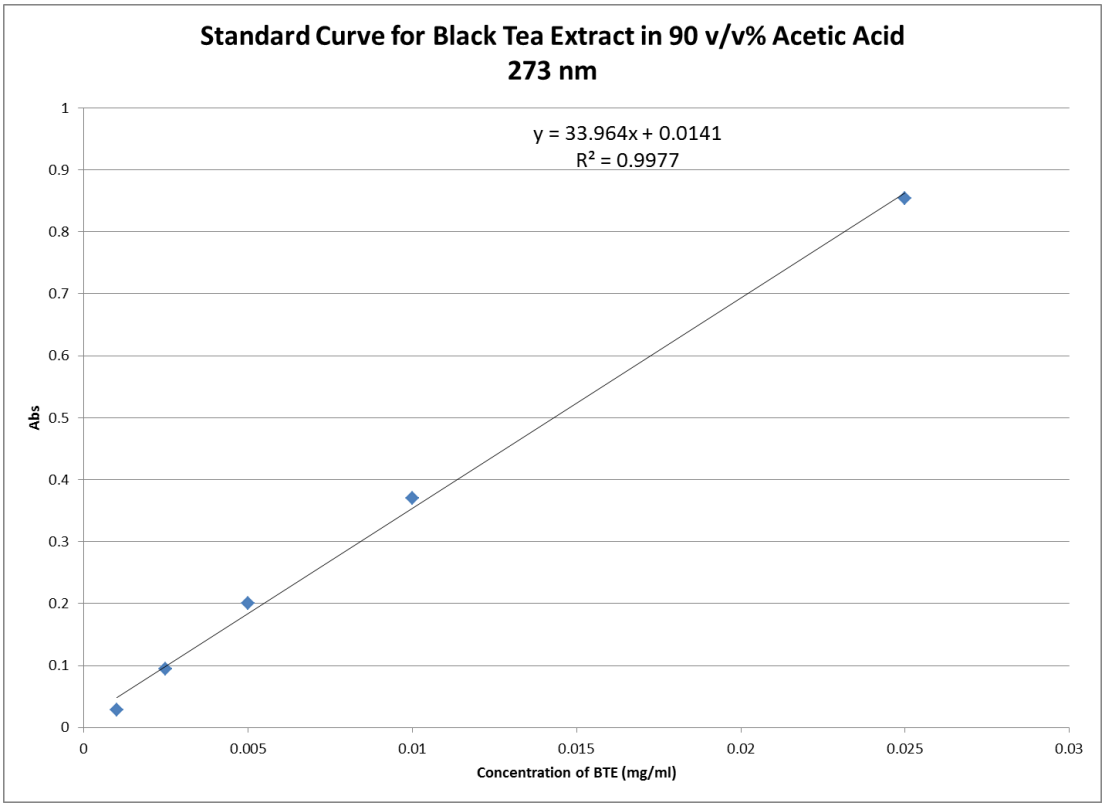

Figure 22. UV-VIS Standard curve for black tea extract in 90% v/v acetic acid. This graph shows the absorption levels of known concentrations of black tea extract and gives us a trend line to calculate BTE concentrations of nanoparticles tested.

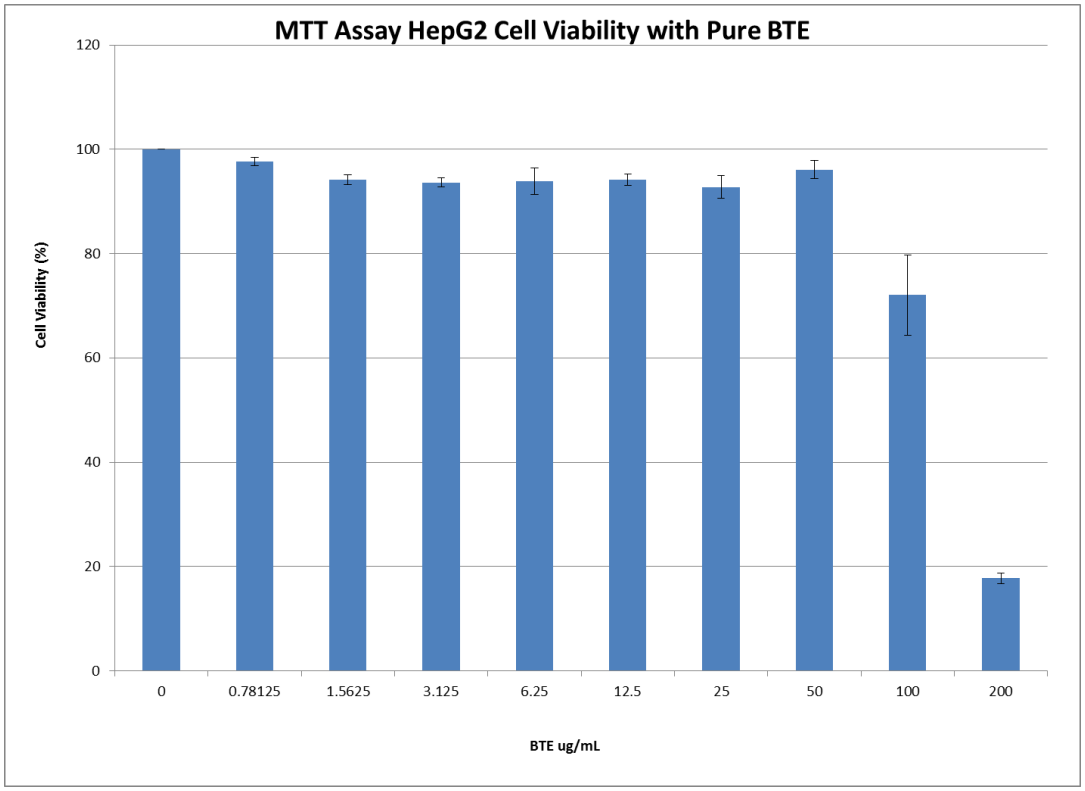

Figure 23. HepG2 cell viability after being treated with varying amounts of pure BTE

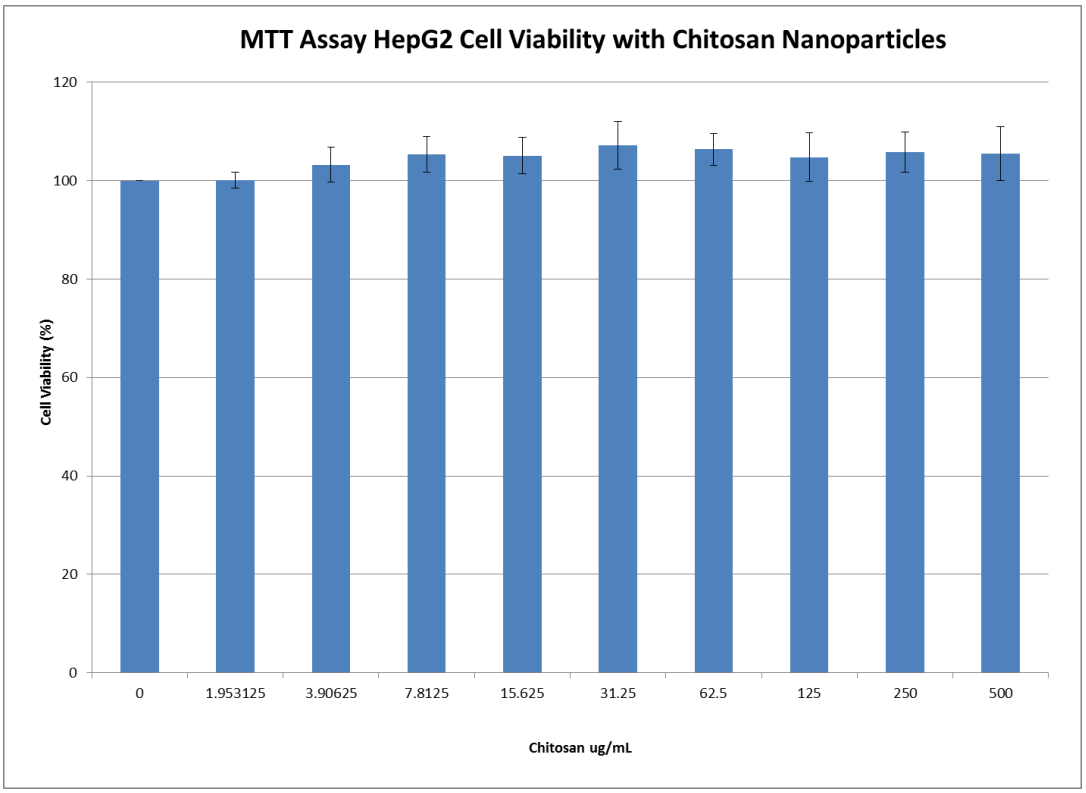

Figure 24. HepG2 cell viability after being treated with varying amounts of chitosan nanoparticles.

Average Diamater of Chitosan Nanoparticles		
	Mean	*Standard Deviation*
5 mg/ml	364.859 nm	131.869 nm
10 mg/ml	443.09 nm	161.643 nm
15 mg/ml	626.232 nm	169.826 nm
20 mg/ml	485.052 nm	239.682 nm
30 mg/ml	512.557 nm	294.525 nm
40 mg/ml	463.034 nm	352.27 nm

Table 1. Average diameter of blank chitosan nanoparticles. One hundred particles were measured for all averages.

Average Diamater of Chitosan-BTE Nanoparticles		
	Mean	*Standard Deviation*
5 mg/ml	429.586 nm	149.844 nm
10 mg/ml	560.521 nm	172.956 nm
15 mg/ml	488.095 nm	360.009 nm
20 mg/ml	326.998 nm	196.881 nm
30 mg/ml	255.594 nm	141.74 nm
40 mg/ml	480.535 nm	285.837 nm

Table 2. Average diameter of chitosan-BTE nanoparticles. One hundred particles were measured for all averages.

Encapsulation Efficiency of Chitosan-BTE Nanoparticles					
	Total Weight(mg)	BTE Weight (mg)	Average Abs	Unencapsulated BTE (mg)	Efficiency
5 mg/ml	1	0.1667	0.081	0.006	96.40%
10 mg/ml	2	0.1818	0.082	0.006	96.70%
15 mg/ml	3.2	0.2	0.088	0.006527	96.70%
20 mg/ml	5	0.23	0.13	0.01	95.50%
30 mg/ml	7.7	0.2484	0.106	0.008119	96.70%
40 mg/ml	7.5	0.1892	0.494	0.04239	76.80%

Table 3. Encapsulation efficiency of chitosan-BTE nanoparticles with varying concentrations of chitosan. The equation $y = 33.964x + 0.0141$ where x is the concentration of BTE and y is the absorbance measured at 273 nm was derived from a standard curve of pure BTE and used to calculate total BTE that was not encapsulated to find efficiency of chitosan-BTE nanoparticles.